Molecular Neurobiology (2020) 57:4031–4044
https://doi.org/10.1007/s12035-020-01995-2

Transition and Dynamic Reconfiguration of Whole-Brain Network in Major Depressive Disorder

Shengpei Wang[1,2] · Hongwei Wen[3,4] · Xiaopeng Hu[5] · Peng Xie[6,7,8] · Shuang Qiu[1] · Yinfeng Qian[5] · Jiang Qiu[3,4] · Huiguang He[1,2,9]

Received: 1 February 2020 / Accepted: 22 June 2020 / Published online: 10 July 2020
© Springer Science+Business Media, LLC, part of Springer Nature 2020

Abstract

Major depressive disorder (MDD) has been characterized by abnormal brain activity and interactions across the whole-brain functional networks. However, the underlying alteration of brain dynamics remains unclear. Here, we aim to investigate in detail the temporal dynamics of brain activity for MDD, and to characterize the spatiotemporal specificity of whole-brain networks and transitions across them. We developed a hidden Markov model (HMM) analysis for resting-state functional magnetic resonance imaging (fMRI) from two independent cohorts with MDD. In particular, one cohort included 127 MDD patients and 117 gender- and age-matched healthy controls, and the other included 44 MDD patients and 33 controls. We identified brain states characterized by the engagement of distinct functional networks that recurred over time and assessed the dynamical configuration of whole-brain networks and the patterns of activation of states that characterized the MDD groups. Furthermore, we analyzed the community structure of transitions across states to investigate the specificity and abnormality of transitions for MDD. Based on our identification of 12 HMM states, we found that the temporal reconfiguration of states in MDD was associated with the high-order cognition network (DMN), subcortical network (SUB), and sensory and motor networks (SMN). Further, we found that the specific module of transitions was closely related to MDD, which were characterized by two HMM states with opposite activations in DMN, SMN, and subcortical areas. Notably, our results provide novel insights into the dynamical circuit configuration of whole-brain networks for MDD and suggest that brain dynamics should remain a prime target for further MDD research.

Keywords Resting-state fMRI · Major depressive disorder (MDD) · Hidden Markov model (HMM) · Brain network dynamic · Transition probability

Shengpei Wang, Hongwei Wen and Xiaopeng Hu contributed equally to this work and should be considered as co-first authors.

Electronic supplementary material The online version of this article (https://doi.org/10.1007/s12035-020-01995-2) contains supplementary material, which is available to authorized users.

✉ Jiang Qiu
qiuj318@swu.edu.cn

✉ Huiguang He
huiguang.he@ia.ac.cn

[1] Research Center for Brain-inspired Intelligence and National Laboratory of Pattern Recognition, Institute of Automation, Chinese Academy of Sciences, Beijing, China

[2] University of Chinese Academy of Sciences, Beijing, China

[3] Key Laboratory of Cognition and Personality (Ministry of Education), Chongqing, China

[4] School of Psychology, Southwest University, Chongqing, China

[5] Department of Radiology, the First Affiliated Hospital of Anhui Medical University, Hefei, Anhui, China

[6] Institute of Neuroscience, Chongqing Medical University, Chongqing, China

[7] Chongqing Key Laboratory of Neurobiology, Chongqing, China

[8] Department of Neurology, the First Affiliated Hospital of Chongqing Medical University, Chongqing, China

[9] Center for Excellence in Brain Science and Intelligence Technology, Chinese Academy of Sciences, Beijing, China

Introduction

Major depressive disorder (MDD) is one of the most prevalent psychiatric disorders, characterized by pervasive depressed mood, anhedonia, cognitive disability, and a high rate of recurrence [1, 2]. It is the second leading cause of disability worldwide, with point prevalence exceeding 4% [3, 4]. Recent researches indicate that abnormal communication among brain systems likely affects multiple cognitive processes directly related to depressive symptoms, and this disrupted brain communication is central to the pathophysiology of the disorder [5–7]. Therefore, understanding communication across brain regions is necessary for the elucidation of the complex mechanisms underlying depression and to guide the development of interventions aimed at improving cognition. Previous researches utilizing resting-state functional magnetic resonance imaging (rs-fMRI) have highlighted that the abnormal functional connectivity (FC) among the cerebral cortex and subcortical areas for MDD [8–10]. However, FC is relatively stable over time and cannot capture the spontaneous fluctuations in brain connectivity [11–13]. Abundant evidence suggests that the human brain is a complex dynamic system that transitions smoothly and continuously through states that directly support cognitive function [8, 14–17]. Further, previous studies have indicated the altered dynamical characterizations, such as dynamical FC or dynamics of intrinsic brain activity in patients with schizophrenia [18–21], Alzheimer's disorder [22, 23], or bipolar disorder [24, 25]. Although dynamic functional connectivity is an emerging area in psychiatry, the altered dynamics of brain connectivity may be an important dimension of the pathophysiology of psychiatric illnesses [11, 26].

The most common technique used for analyzing brain network dynamics is the use of sliding windows for resting state [27–30]. Recent studies based on this approach indicate that global synchronization and temporal stability were significantly increased in the MDD patients and variability of functional connectivity within DMN and FPN were significantly decreased [31, 32]. The MDD patients displayed decreased FC between medial prefrontal cortical (mPFC) and regions of para-hippocampal gyrus within the default network and increased dynamic FC between mPFC and regions of insula [33]. Although these findings based on the sliding windows approach have complimented the abnormal dynamics of the brain for depression, this approach has some limitations [11, 26, 34–36]. Specifically, the observed neural processes of interest are highly dependent on the pre-specification of the time-scale such as the temporal width of the window and the length of the step. The choice of the window width is crucial because a long window will limit the visibility of fast time-scale and a short window length will provide insufficient data for a reliable network estimation.

However, the hidden Markov model (HMM) approach can overcome the above limitation of the sliding window approach [37]. The HMM does not require pre-specification of sliding window length; instead, the relevant time-scales are acquired directly from the data [37–39]. The HMM describes brain activity as a dynamic sequence of discrete brain states in a data-driven manner. Each HMM state is characterized by a distinct pattern of network activity, including functional connectivity and spectral content [37–39]. Previous studies confirm that the HMM is capable of identifying dynamic reorganization of the whole-brain network on minimal time scales [39–42]. The applications of HMM-based on magnetoencephalography (MEG) have shown state switching between large-scale networks in as little as 100 ms [40–42]. Hence, the HMM methodology has been proven useful in task data and resting-state data. In particular, based on resting data [39], the HMM can be capture quasi-stationary states of activity that are consistently recurring over a population of humans. This allows for the analysis of how certain dynamic properties vary across subjects, such as the transition probabilities between states or the differences of state occupancies (the temporal proportion of a recording in which an HMM state was active). Previous studies prove that during rest, the dynamics of whole-brain resting-state networks can be characterized in MEG and fMRI and discovered that the transitions between states or networks are far from random [29, 39–42]. Thus, the HMM can provide a rich description of brain network dynamics and can describe the switching dynamics of large-scale brain networks on short timescales.

In this study, we employed an HMM analysis to identify the recurring brain states from rs-fMRI from two independent cohorts with MDD. We aim to investigate the complicated temporal dynamics of brain activity and to characterize the spatiotemporal specificity of whole-brain networks for MDD. Furthermore, we also examine whether there is a specific pattern of transitions across states for MDD and controls.

Materials and Methods

Participants

Our study included two independent cohorts, one from the First Affiliated Hospital of Chongqing Medical University (F-CQMU), and another from the Anhui Mental Health Centre (AMHC). Notably, data from the F-CQMU cohort were considered in the main analysis, which consisted of 127 participants with MDD (F/M 83/44; mean age (standard deviation, SD) 38.32 ± 13.76 years) and 117 age- and sex-matched healthy controls (F/M 74/43; mean age (SD) 38.89 ± 14.14 years) [43]. Data from the AMHC cohort was considered in the validated analysis to improve the reproducibility of the main analysis, which consisted of 44 participants with

MDD (F/M 32/12; mean age (SD) 37.30 ± 8.95 years) and 33 age- and sex-matched healthy controls (F/M 24/9; mean age (SD) 38.50 ± 11.25 years). Across cohorts, all participants underwent a diagnostic interview independently by experienced psychiatrists according to the Structured Clinical Interview for the Diagnostics and Statistical Manual of Mental Disorders. All met identical neuroimaging exclusion criteria (SI Methods), which were derived from previous studies [43, 44]. The study was conducted with approval from the Institutional Review Board of Chongqing Medical University (No. 2016121) and Anhui Mental Health Center Research Ethics Committee (No. 201410072) and was performed following the Declaration of Helsinki. Written informed consent was obtained from all participants.

Additionally, the T1-weighed high-resolution MRI scan and the fMRI scan were acquired for each participant across cohorts. All MRI data underwent identical preprocessing and quality assurance and analyses. The scan parameters and full details of preprocessing were provided in SI Methods.

Hidden Markov Model

To investigate the dynamic whole-brain networks in a data-driven manner, we applied HMM to time courses extracted from the cortical and subcortical areas. Previous researches indicate that different observation distributions can be adequate for different data modalities [29, 37, 38, 42]. The most common variety of the HMM uses a multivariate Gaussian observation model, typically characterizing the distribution of each state by an activation map and a covariance matrix [37]. Full details are provided in SI Methods. Here, we applied independently the HMM with a multivariate Gaussian distribution to fMRI data from each cohort, such that we obtained the independent group estimation of the states. Additionally, we applied the HMM on the F-CQMU dataset as the main analysis and considered the analysis on the AMHC dataset as the validated analysis. The steps of the main HMM analysis were as follows (Fig. 1): First, we parcellated the whole-brain regions into 90 regions of interest (ROIs) according to the Automated Anatomical Labelling (AAL) [45] for each participant. Then, we averaged the time courses over all voxels with ROIs and obtained the representative time courses of 90 regions for each subject. Next, the participant-specific set of 90 ROI time courses were demeaned, divided by their standard deviation, and concatenated across participants, yielding a data matrix of dimensions 90*(244*232) with 232-time points. Finally, the HMM inference estimated the number of recurring discrete states according to the demeaned time courses, each of which was characterized by a unique configuration of data statistics. Each recurring state was modeled as a multivariate normal distribution with first (mean activity) and second-order statistics (covariance matrix) [29, 37]. In the HMM analysis, the HMM inference identified periods of quasi-stationary activity, where the 90 ROI time courses could be described by certain configurations of mean activity and FC.

Analysis of Dynamics and Transitions of HMM States

Based on the inferred HMM, we estimated a range of statistics reflecting the properties of the HMM state. Global characterizations about the HMM dynamics were estimated from the time course of posterior probabilities, which are potentially more sensitive to cases where two or more states are approximately equally probable [38, 40]. Fractional occupancies of HMM states are computed as the temporal proportions of recording, in which an HMM state is active. The lifetime is the amount of time spent in a state before moving into a new state, and interval time is computed as the amount of time between consecutive visits to a state [38, 40]. These characterizations can effectively capture the within-subject temporal dynamics.

Furthermore, to investigate common brain states in the matrix of transition probabilities, we used a network-based clustering technique known as community detection. The HMM states of communities expressed more frequent transitions within each other than to states outside. In particular, we chose a common community detection approach known as modularity maximization, where the following modularity quality function is optimized using a Louvain-like locally greedy heuristic algorithm [46, 47]. Before running the modularity algorithm, we thresholded the transition matrix to include the strongest elements and included 21% of the strongest transitions according to the previous study. However, different thresholds resulted in highly similar module partitions.

Statistical Analysis

We performed respectively two-tailed two-sample t tests to test for significant differences of global dynamics of HMM states between patients with MDD and healthy controls for each scan site. In particular, gender, age, and education were considered irrelevant variables and be regressed out to remove their effects. We performed non-parametric permutation testing to investigate the transition probability of HMM states between patients with MDD and healthy controls. By running 5000 permutations across patients with MDD and controls, we effectively created a null distribution for global dynamics of each state of differences between groups, which we then used to produce p values. For all statistical analysis, the threshold $p < 0.05$ and false discovery rate (FDR) correction was set to determine the significance level.

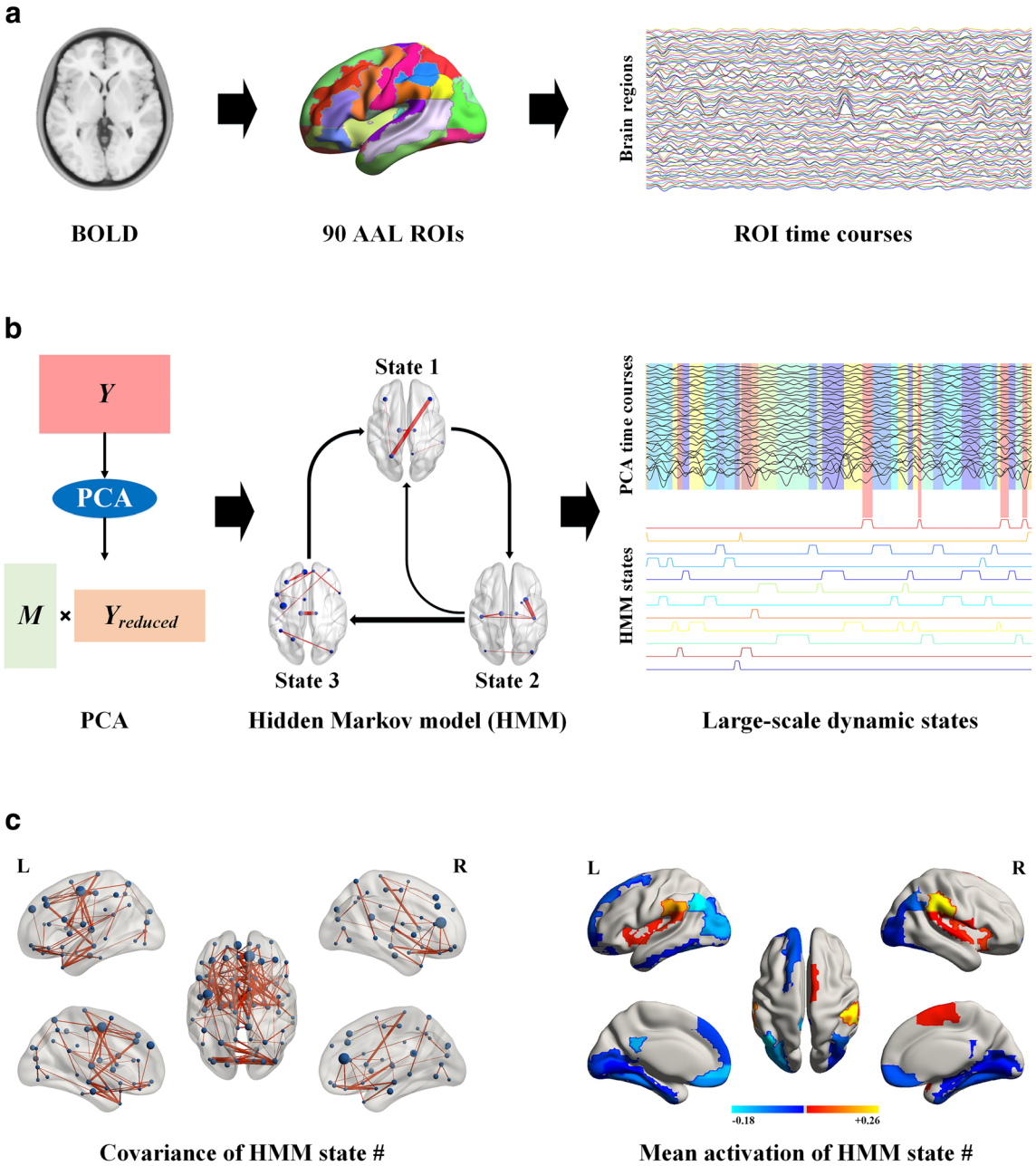

Fig. 1 Schematic illustration of dynamic whole-brain networks using a hidden Markov model (HMM). **a** The ROI time series were extracted by averaging BOLD signal across voxels within each ROI for each participant. Each time series of ROIs was demeaned and normalized using its standard deviation. **b** The data were concatenated across all subjects including MDD and CN groups. Next, the principal component analysis (PCA) was used to reduce the dimensionality of the data. Then, the HMM was run on the PCA-reduced time series, resulting in the K number of states with associated time series. **c** Each HMM state was characterized by a multivariate Gaussian distribution comprising a covariance matrix and a mean distribution

Validated Analysis

Robustness is the key issue in the HMM analysis. To improve the reproducibility of the main analysis, we underwent an identical HMM analysis for the AMHC data. First, we performed the same steps of HMM analysis and estimated HMM states independently in the AMHC data. Then, we computed the fractional occupancies, lifetime, and interval time of each HMM state and performed two-tailed two-sample *t* tests to test between participants with MDD and controls. Next, we investigated the spatial activation maps of the specified HMM states for MDD. Finally, we estimated the similarity between states across cohorts using the Bhattacharyya distance.

Results

Demographic and Clinical Characteristics

For the F-CQMU data, there were no significant differences between the healthy control and MDD disease group in terms of gender ($p = 0.731$, Fisher's exact test), age ($p = 0.749$, two-tailed two-sample t test) and education ($p = 0.0897$). Meanwhile, compared with controls, the scores of neuroticism were significantly increased for MDD ($p < 0.001$) and the extroversion scores were significantly decreased ($p < 0.001$). Additionally, other clinical characteristics for MDD, including HAMA, HAMD, and BDI-II scores, were also recorded and evaluated (Table S1). For the AMHC data, there were also no significant differences between MDD and controls in terms of gender and age. Demographic and clinical characteristics across cohorts are shown in Table 1.

Large-Scale Brain Network States Identified by HMM

To probe the alteration of the inherent large-scale networks, we estimated an HMM on resting-state fMRI data from the F-CQMU data. We evaluated the different number of HMM states by some summary statistics, including minimum free energy and medial fractional occupancy across the HMM states (Fig. S2–3 in SI Results). Specifically, the minimum free energy was monotonically decreased over the large numbers of tested states. The median fractional occupancy across HMM states was decreased as the number of states was increased and ceased around the number of states for 12. A similar phenomenon is also reflected in the development of the average lifetime. Hence, based on HMM, we estimated 12 states without any information regarding depression for its estimation. Each estimated HMM state was defined as a multivariate Gaussian distribution, including a mean activation distribution and an FC matrix (Fig. S4–5).

Alterations of Dynamics for each HMM State for MDD

Together with the state distribution, the HMM inference also estimates the time courses of the visits to each of the brain states. We used the fractional occupancies, lifetimes, and interval times of HMM states to probe the temporal characteristics of MDD. Compared with CN, fractional occupancies of HMM states 1, 2, and 11 of participants with MDD were significantly decreased (state 1: $p = 0.0053$; state 2: $p = 0.0027$; state 11: $p = 0.0305$, two-sample t test). Fractional occupancies of HMM states 3, 7, and 9 were significantly increased (state 3: $p = .001$; state 7: $p = 0.001$, state 9: $p = 0.0446$) (Fig. 2a). The fractional occupancies of the remaining HMM states displayed no significant differences between controls and MDD patients. Lifetimes and interval time of participants with MDD had a similar alteration with fractional occupancies. The HMM states 3 and 7 generally expressed longer lifetimes (state 3: $p = 0.001$; state 7: $p = 0.0021$) and HMM states 1, 2, and 11 expressed shorter lifetimes (state 1: $p = 0.0210$; state 2: $p = 0.0051$; state 11: $p = 0.0267$) (Fig. 2b). The interval times of HMM states 3, 7, and 8 were significantly increased for participants with MDD (state 3: $p = 0.0319$; state 7: $p = 0.0012$; state 8: $p = 0.0003$) and interval times of HMM state 12 was significantly decreased ($p = 0.0320$) (Fig. 2c). Our results indicate special patterns of the temporal configuration of large-scale brain networks in MDD, which are characterized by the reorganization of brain microstates at a time scale.

Significant Alteration of Transition Patterns Between HMM States

To investigate the different transition probabilities of the HMM states, we further compared the transition probability of HMM states between MDD and CN using permutation analysis (5000 permutations). We found no significant

Table 1 Demographic and clinical characteristics of major depression disorders (MDD) and healthy controls (CN)

	F-CQMU		AMHC	
	MDD	CN	MDD	CN
Number of subjects	127	117	44	33
Gender (M/F)	44M/83F	43M/74F	12M/32F	9M/24F
Age (mean ± SD, years)	38.32 ± 13.76	38.89 ± 14.14	37.30 ± 8.95	38.50 ± 11.25
Age range (years)	12–74	19–72	12–51	18–62
Education (years)	11.98 ± 3.63	12.88 ± 4.57	–	–
Duration (months)	49.44 ± 62.65	–	–	–
HAMA	23.40 ± 7.55	–	13.27 ± 5.17	–
HAMD	20.61 ± 5.18	–	21.66 ± 4.47	–
BDI-II scores	19.73 ± 7.97	–	–	–

HAMA Hamilton Anxiety Scale, *HAMD* Hamilton Depression Scale, *BDI-II scores* Beck Depression Inventory-II

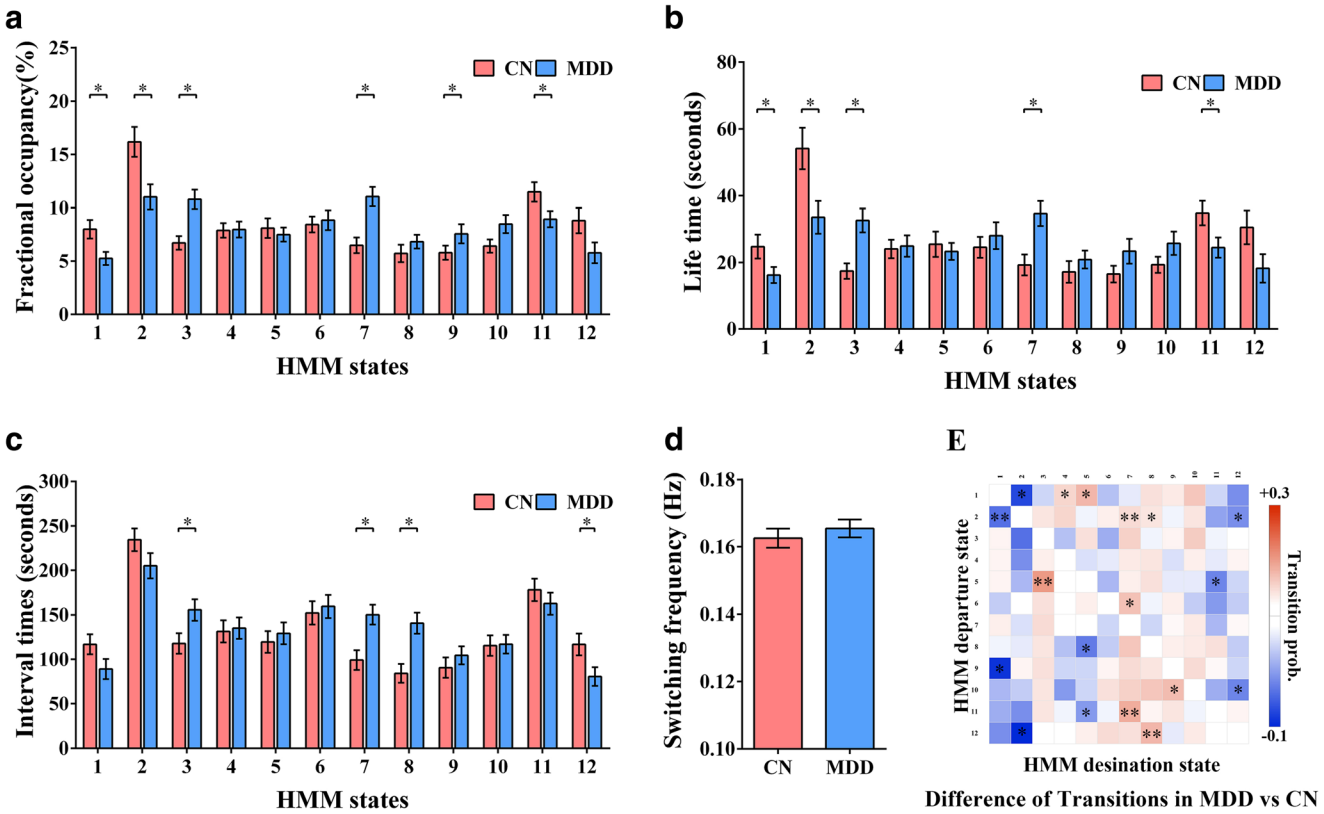

Fig. 2 Alteration in whole-brain network dynamics between MDD and CN in F-CQMU dataset. **a** The significant alteration in fractional occupancies (FO) of each state. **b** The significant alteration in lifetimes (LT) of each state. **c** The significant alteration in interval times (IT) of each state. Error bar represents standard error of the mean (SEM). The different colors represented the different groups (red: CN and blue: MDD). All temporal properties were evaluated using a two-tailed two-sample *t* test and permutations. *Significant difference between the different groups ($p < 0.05$). **d** Switching frequency of MDD and CN in the F-CQMU dataset. **e** The significant alteration of transition probability between MDD and CN. Red represents the significant increase in MDD compared with CN, and blue represented a significant decrease in MDD compared with CN. Significant differences between the two groups were evaluated using a permutation test with 5000 permutations and denoted by asterisks: $*p < 0.05$; $**p < 0.005$

difference in switching rate between MDD and CN (Fig. 2d), suggesting that there are similar stable network dynamic patterns in the entire scan process between MDD patients and controls. However, we found significant group differences in switching probability between HMM states (Fig. 2e). Compared to controls, the switching probabilities from HMM state 5 to 3, from states 2 and 11 to 7, and from state 12 to 8 increased significantly for MDD (state 5 to 3: $p < 0.001$; state 2 to 7: $p = 0.0012$; state 11 to 7: $p = 0.0016$; and state 12 to 8: $p = 0.0036$). The switching probability from HMM state 2 to 1 significantly decreased for MDD ($p = 0.0024$). Given these results, the significant alteration of transition between HMM states for MDD patients suggests that the transition pattern and communication between brain network states were significantly altered.

The Specific Community Structure of Transitions for MDD

We further examined the transition patterns of HMM states, extracting modules of HMM states that transition more often between each other than to other states (Fig. 3a). Combined with the global statistics and community structure of transitions (Fig. 3b), we found three modules in transition map, respectively, as CN-related module (red), MDD-related module, and the shared module by MDD and CN (Fig. 3c). Specifically, states in the CN-related module had higher fractional occupancy and lifetime in controls, while states in the MDD-related module had higher global temporal statistics in participants with MDD. In the shared module, some states had higher statistics for controls and other states had higher

Fig. 3 Investigating modules of transitions between states for the F-CQMU dataset. **a** The probability matrix of the 12 HMM states across all participants. Each matrix entry represented the transition probability from departure states to destination state. **b** Three modules of the 20% strongest transitions of the HMM states. **c** The transition map with each HMM state. Arrows showed the direction of the transitions with thickness proportional to the transition probability. **d** Mean activation distribution of the CN-related HMM states. **e** Mean activation distributions of the shared HMM states. **f** Mean activation distributions of the shared HMM states. All maps were thresholded respectively above the 50% strongest positive and below negative changes

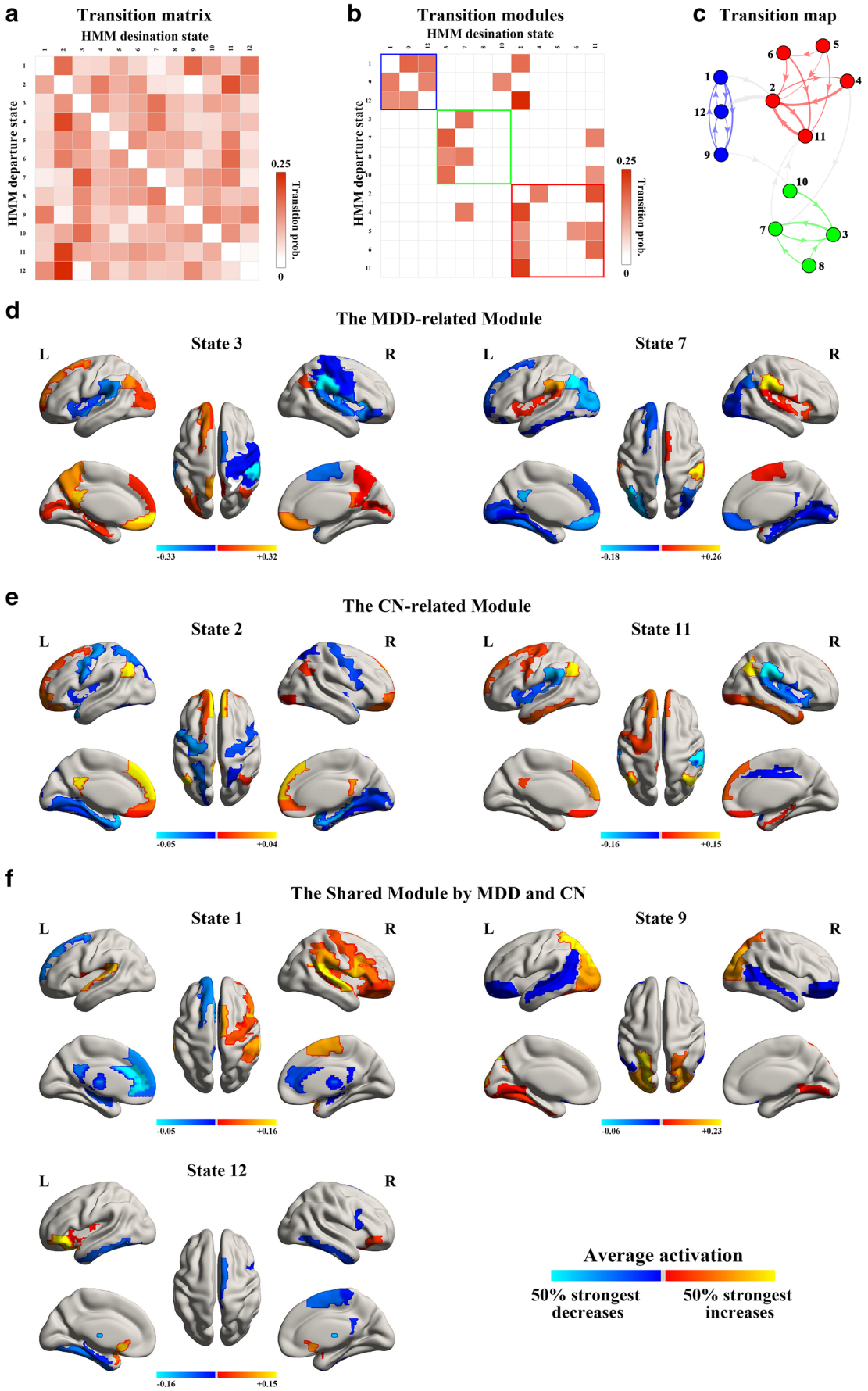
a
Transition matrix
HMM desination state
HMM departure state
0.25
Transition prob.
0
b
Transition modules
HMM desination state
HMM departure state
0.25
Transition prob.
0
c
Transition map
d
The MDD-related Module
State 3
L
R
-0.33
+0.32
State 7
L
R
-0.18
+0.26
e
The CN-related Module
State 2
L
R
-0.05
+0.04
State 11
L
R
-0.16
+0.15
f
The Shared Module by MDD and CN
State 1
L
R
-0.05
+0.16
State 9
L
R
-0.06
+0.23
State 12
L
R
-0.16
+0.15
Average activation
50% strongest decreases
50% strongest increases

statistics for patients with MDD. There were more frequent transitions across states in the shared module. The CN-related module was characterized by states 2 and 11 with higher global temporal statistics for controls and the MDD-related module by HMM states 3 and 7 with higher global temporal statistics for MDD participants. The module shared by MDD and CN was characterized by HMM state 1 with higher statistics for controls and HMM state 9 with higher statistics for MDD. Further, the HMM states across the different modules exhibit a strong directed structure. The shared module may have transferred toward MDD-related module from HMM states 9 to 10 and toward CN-related module from states 1 and 12 to 2. The CN-related module transferred toward MDD-related module from state 4 to 7. Alternatively, the MDD-related module transferred toward CN-related module from HMM states 7 and 10 to 11. The organization of the transition modules indicates the special module of brain networks for MDD and the multiple transition pathways between MDD and CN.

Spatial Activation Maps of Whole-Brain States

We finally probe the spatial activation maps of the large-scale whole-brain network states in different modules. First, the CN-related module is mainly characterized by states 2 and 11 (Fig. 3d). The HMM state 2 showed the decreased activation in subcortical areas (including the right amygdala, bilateral pallidum, bilateral para-hippocampal gyrus, and bilateral putamen) and sensory and motor areas (including bilateral fusiform gyrus, lingual gyrus, superior parietal gyrus, and precentral gyrus), and the increased activation in DMN (including the bilateral medial and superior frontal gyrus and left PCC). The HMM state 11 showed decreased activation in the bilateral insula, bilateral middle cingulate cortex, and the bilateral superior temporal gyrus, and increased activation in bilateral angular, left PCC, bilateral superior and medial frontal gyrus, left precentral gyrus, and bilateral inferior temporal gyrus. Second, the MDD-related module (green) is dominated by states 3 and 7 (Fig. 3e). The main decreases of HMM state 3 were observed in the key areas of the bilateral insula, superior temporal gyrus, and superior marginal gyrus and left precentral gyrus and the increase was in subcortical areas (including bilateral angular, left hippocampus and para-hippocampal gyrus) and DMN areas (including the bilateral precuneus, left superior and medial frontal gyrus, bilateral PCC, and calcarine cortex). The HMM state 7 had the inverse activation pattern with state 3, showing the decreases in some areas (including bilateral angular, para-hippocampal gyrus fusiform gyrus, superior and medial frontal gyrus, middle and inferior occipital gyrus, and bilateral lingual gyrus) and the increases in bilateral insula, superior marginal gyrus, and superior temporal gyrus. Finally, the module shared by MDD and CN consists of HMM states 1 and 9 (Fig. 3f). The HMM state 1 demonstrated the majority of decreased activation in subcortical areas (including the bilateral hippocampus, thalamus, and left amygdala) and right anterior and PCC, and increased activation in motor and sensory network (including bilateral inferior and superior temporal gyrus, right precentral gyrus, and supplementary motor areas). The HMM state 9 demonstrated decreased activation in the orbitofrontal gyrus and increased activation in visual and lingual areas (including the bilateral lingual gyrus and the bilateral middle superior occipital gyrus). Combined with the special community structure of transitions, we found that patients with MDD and healthy controls displayed antithetical activation patterns in the key areas of DMN and sensorimotor networks. The transitions of states in the shared module toward other modules follow this antithetical pattern of activation in DMN and sensorimotor networks.

Validated Analysis of the AMHC Data

To investigate the reproducibility of HMM states in the F-CQMU data, we underwent the identical HMM analysis for the independent AMHC dataset. Based on the size of data and evaluation of the state number as above (Fig. S3), we identified six HMM states (Fig. S6). Then, we found similar results in global dynamic characteristics for the AMHC dataset, including fractional occupancy, lifetime, and interval time (Fig. 4a–c). Specifically, compared to controls, fractional occupancy of HMM state 5 was significantly increased for MDD patients ($p = 0.0268$) and fractional occupancy and lifetimes of State 6 were significantly decreased (fractional occupancy: $p = 0.0011$; lifetimes: $p = 0.0014$). Additionally, interval times of both states 5 and 6 were significantly increased (state 5: $p = 0.0109$ and state 6: $p = 0.05$). Further, we examined the spatial activation maps of HMM states and found similar results. Particularly, the state 5 was observed the decreases in the visual network (including the bilateral occipital gurus) and the increases in subcortical areas (including the bilateral insula, bilateral putamen, left pallidum, and bilateral caudate) (Fig. 4d), which was the most similar to the states 3 and 7 of the MDD-related module in F-CQMU dataset (Bhattacharyya distance: state 3 = 0.6569 and state 7 = 0.6935). The state 6 showed the decreased activation in subcortical areas (including the right amygdala, the bilateral insula, right putamen, and hippocampus) and sensory network (including the bilateral temporal gyrus and para-cingulate cortex) and increases in the bilateral angular and orbitofrontal gyrus (Fig. 4e), which was the most similar to the CN-module states in F-CQMU dataset (Bhattacharyya distance: state 2 = 0.5698 and state 7 = 0.6169). In summary, our findings suggest the robustness of the main analysis and dynamic reconfiguration of states in MDD participants across cohorts.

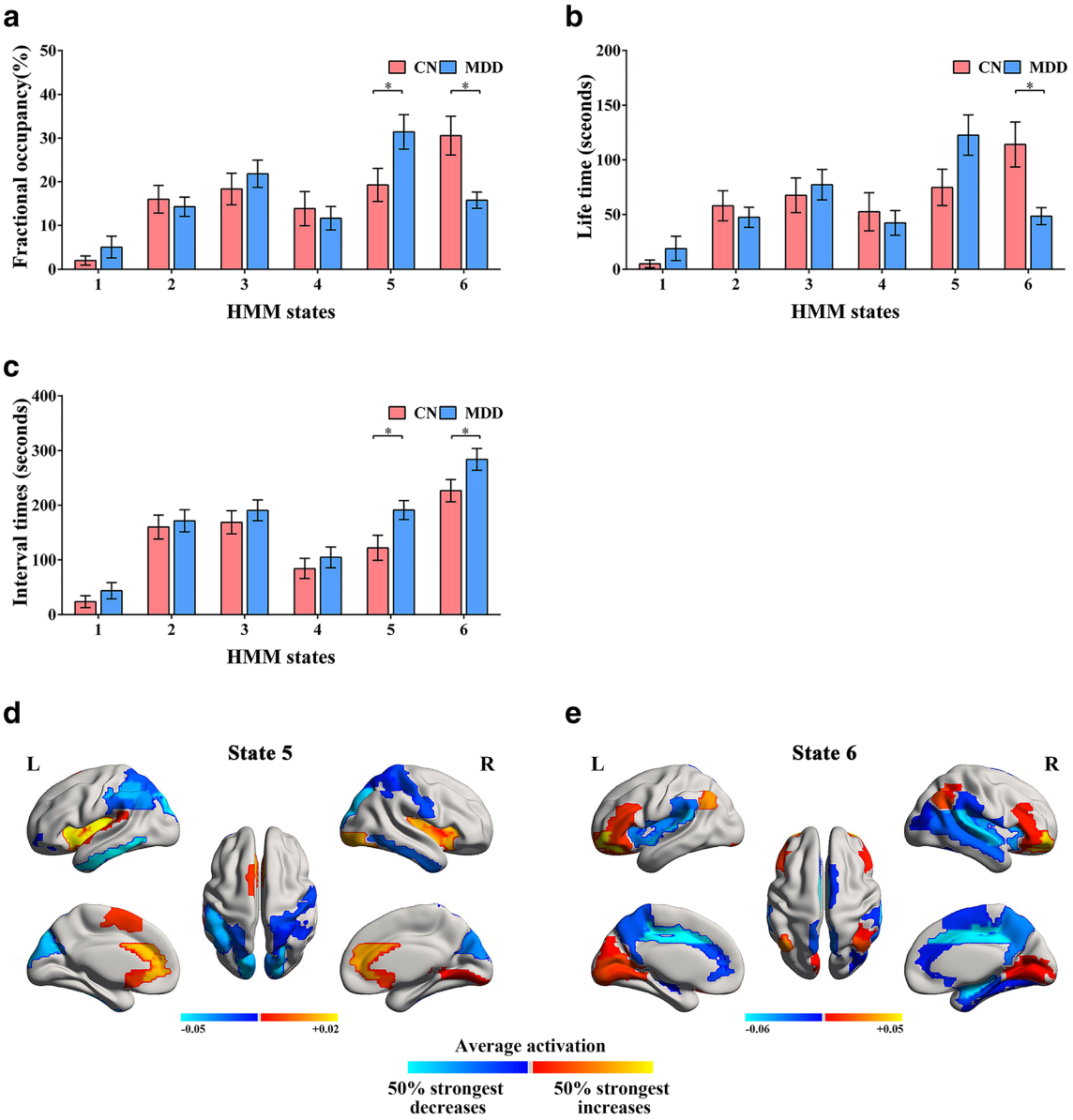

Fig. 4 Alteration in whole-brain network dynamics between MDD and CN in AMHC dataset. **a** The significant alteration in fractional occupancies (FO) of each state. **b** The significant alteration in lifetimes (LT) of each state. **c** The significant alteration in interval times (IT) of each state. Error bar represents standard error of the mean (SEM). The different colors represented the different groups (red: CN and blue: MDD). All temporal properties were evaluated using a two-tailed two-sample *t* test and permutations. *Significant difference between the different groups ($p < 0.05$). **d**, **e** Mean activation distribution of states 5 and 6. All maps were thresholded respectively above the 50% strongest positive and below negative changes

Discussion

Based on the data-driven approach in large-scale whole-brain networks, we explored the rich dynamic complexity and dissimilarity in spatiotemporal patterns of brain activity between MDD and controls across cohorts. We used the HMM to extract 12 recurring brain states from all subjects in the F-CQMU cohort. Each HMM-derived whole-brain network state was characterized in space by the patterns of mean activation in time by the probability of being active at each time point [37]. Comparing the temporal evolution of the HMM-derived states between MDD and controls, we discovered the temporal reconfiguration of brain networks underlying depressive disorder, which provides a better temporal description than previous studies using the slide window approach. Then, the community analysis of the HMM transition map revealed a specificity and abnormality of large-scale network activity in MDD participants, which previous studies did not fully capture. Finally, we adopted the identical HMM analysis in the AMHC cohort to suggest the robustness of the HMM states and the dynamic reconfiguration of states for MDD across datasets.

Significant Alteration of Whole-Brain Dynamics in MDD

Previous studies indicate that fMRI can be used to identify dynamic re-configurations of large-scale brain activity for depression voxel-wise changes in activity [48], changes in connection strength [9, 49], or through long-temporal dependencies in the blood oxygenation level dependent (BOLD) signal [32, 33]. The HMM analysis is a probabilistic representation in the space of whole-brain network states and transitions. Here, we identified 12 HMM states for large-scale brain networks across patients with MDD and healthy controls, consistent with previous findings that functional connectivity in the human brain is highly dynamic, representing flexibility in functional coordination between distinct brain systems [31–33]. Further, we analyzed the time course of visits to each HMM state of large-scale brain networks and found the temporal reconfiguration of whole-brain networks for MDD. Our findings are consistent with previous findings that MDD patients and controls remained indifferent overall brain states for significantly different periods. Previous researches utilizing dynamical functional connectivity indicate that compared to controls, MDD patients were associated with increased mean dwell time and decreased FC between and within subnetworks (including cognitive control network and DMN) in the weakly connected state [31, 33]. Recent studies also suggest that MDD displays significantly lower dwell time and fraction time for the states [32, 50], which was characterized by the low modularity, hyper-connectedness of sensory-related regions and DMN, and weak connections between cortical and subcortical areas. Besides, other researches on other psychiatric illnesses suggest that the dwell time of the brain states was the crucial feature explaining neurological mechanisms that underlay psychiatric illnesses [25, 26, 51, 52]. Previous studies suggest that schizophrenia patients spend much less time than healthy controls in states typified by strong large-scale connectivity [18, 19, 51]. Some studies also report differences in the dwell time within different subnetwork configurations of the DMN between Alzheimer's patients and age-matched healthy controls [53–55]. The mean dwell time and the fraction of one globally hypoactive state accounted for the high proportion of brain activities which were significantly increased in patients with a generalized anxiety disorder (GAD) [52]. In summary, our results provide new insights about the temporal features in depression and offer potential biomarkers for the evaluation of the impacts of psychiatric diseases.

Specific Community Structure of HMM State Transition for MDD

The human brain is a complex dynamic system that transitions smoothly and continuously through states that directly support cognitive function [15, 16]. Understanding these transitions is critical for our understanding of functional brain plasticity. Hence, based on 12 HMM-driven states, we analyzed the switching rate of the HMM states defined as the frequency of transitions between states. Consistent with previous studies [31–33], we observed that the switching rate of brain states for MDD was slightly higher than that in healthy controls but there were no significant differences with controls. Our findings suggest that MDD exhibits a stable pattern of transitions across brain networks, which is similar to controls.

Based on the community detection for the transition map and combined with the global dynamics of large-scale brain networks, our results indicate that patients with MDD and controls have their specific community structures in the transition map of the HMM states. In particular, there were the special modules of transitions respectively related to MDD and controls. The MDD-related module was characterized by the opposite activations in DMN, sensory and motor network (SMN), and subcortical network. The CN-related module was characterized by the decrease of subcortical areas and the increase of DMN (including PCC, superior and medial frontal gyrus, and inferior temporal gyrus). Our findings are consistent with previous studies on depression that suggest the abnormal connection of DMN is the crucial characteristic of MDD [4, 56, 57]. A voxel-wise meta-analysis of 32 previous studies revealed increased orbitofrontal DMN FC and decreased FC between the dorsomedial prefrontal cortex and posterior DMN in MDD [4]. One recent study based on an unprecedentedly large sample also found the decreased FC within the DMN in MDD compared with controls and the alterations in FC of visual, sensory motor, and dorsal attention networks in MDD [4].

Notably, we observed a module shared by MDD and CN, which previous studies did not fully capture. The module was characterized by the decrease in subcortical areas, cingulate cortex and orbitofrontal gyrus, and the increase of the inferior and superior frontal regions and sensory areas. Additionally, we found that the shared module has strong triangular loops of transitions and the strongly directed transitions to the CN-related or MDD-related modules. In particular, the HMM states in the shared module transited to the MDD-related module from states 9 to 10. In other words, the state characterized by an increase of sensory areas transited to the states characterized by decreases in sensory areas. The shared module transited to the CN-related module from states 1 and 12 to state 2, indicating that the state characterized by a decrease of DMN (anterior and posterior cingulate cortex) transited to the states characterized by increases in DMN. Our findings are consistent with previous studies in that the relationship between posterior default mode network and medial frontal cortex changed from negative to positive in MDD patients after electroconvulsive therapy (ECT) [58–61]. This stable and directed configuration of

transition may be crucial for understanding the neurological mechanisms of and treatment for depression.

Methodological Considerations

The HMM provides a rich description of brain network dynamics, without the limitations of sliding-window approaches [37–39, 41]. More specifically, the HMM decomposes data efficiently and automatically by inferring adaptive data segments for each state and estimating the connectivity across visits to that state. Most information contained in the data was potentially captured as the number of inferred HMM states increased. The HMM approach removes the necessity of being bound to a predefined timescale (the width of the window) and removes any estimation problems of the sliding window approach (i.e., the uncertainty of an estimation based on just a few data points). However, the limitations of the current study should be considered.

First, the HMM makes two assumptions that require some consideration when applied to brain activity data. One assumption of the HMM is that the states are mutually exclusive [37, 41]. Although the inferred state assignments are probabilistic such that the states can share the responsibility of explaining every time point, only one state is assumed to activate at each given time point. In theory, this assumption might limit the number of possible expressible patterns to the number of HMM states. Another assumption in the HMM is the Markovian assumption. When the state at certain time points is known, the state in the next time point will be predicted without needing to know the state time courses before this time point. Therefore, the dependency between state occurrences decays exponentially with time and does not reach very temporally distant data, which is knows as a short-range dependency. There is good evidence that the brain exhibits long-range dependency, so the HMM has potential limitations for precisely characterizing the brain state. However, recent research indicates that the HMM is capable of inferring a certain type of long-range time dependencies in the form of meta-states, even when these are not explicitly parameterized in the model [29, 38, 39, 41]. In summary, although the HMM does not model long-range dependency, it does not prohibit it; in other words, the inferred HMM state sequence is free to discover long-range dependencies inherent to the data.

Second, the number of states of the HMM was a free parameter. Here, the number of HMM states was set at 12 for the F-CQMU cohort and 6 for the AMHC cohort, based on an evaluation of a range of HMM solutions with a varying number of states. It is important to note, however, that it is difficult to determine a correct number of states when decomposing continuous recordings of brain activity. Previous studies suggest that neither slide windows approach nor HMM can be used to decompose the explicit number of intrinsic states from brain activity [11, 34, 38, 39]. We aimed to extract as much temporal resolution as possible from the ROI time courses. Ideally, a higher number of states should provide more temporal detail; however, increasing the number of states was associated with a higher occurrence of sporadic HMM states, modeling very specific subparts of the data and not generalizing across participants. Given this, it is important to emphasize that we do not suggest the number in our study as definitive, but simply as a tool to resolve as much temporal information as possible from the current data.

Third, we regressed out the white matter (WM) signal in data pre-processing to focus on the gray matter (GM) signals, which was the more common step of pre-processing in most study of fMRI. This might be a limitation of our study because of the removal of WM signal. More and more evidences suggested that BOLD signal in the brain WM cannot be attributed simply to noise [62]. The current studies found that brain activation in WM has been detected using BOLD-fMRI [63] and that the brain's WM functional connectome architecture includes small-world topology, high-degree hubs, and a non-random modular organization [64]. These current findings offer evidence for a previously unappreciated WM connectome and elucidating our understanding of WM functional information in both healthy individuals in cases of clinical disease [64]. Although BOLD signals have been robustly detected in brain GM in a large number of studies, whether such signals reliably arise in WM remains controversial. Fundamentally, the biophysical origins of BOLD signals in WM are not clear, along with whether neural signal in WM triggers changes in BOLD signals similar to GM [65]. Therefore, we regressed out the WM signal in data pre-processing to focus on the GM signals, which was the more common step of pre-processing in most study of fMRI. This might be a limitation of our study because of the removal of GM signal. We will explore the dynamics of WM signals in our future work.

Finally, one of the most common treatments for depression is medication, but different drugs have different effects on different people. In our study, 59 of 127 MDD patients from the F-CQMU cohort were medicated and 68 MDD patients were not medicated before the time of fMRI investigation, which might limit our findings. The drugs mainly included escitalopram, mirtazapine, fluoxetine, paroxetine, and so on. The details for medicated participants were shown in Table S3. Therefore, we further explored the differences of global dynamics between unmedicated depression patients and medicated depression patients. We found that there were significant differences in state 7 for fractional occupancy ($p = 0.03$, $t = -2.19$) and life times ($p = 0.457$, $t = -2.02$), and there were no significant differences in remaining states for global dynamics. The details are shown in Fig. S7. In addition, all participants with MDD from the AMHC cohort were not medicated before scanning. Although there were significant

differences in a state, other factor, including course of disease, course of medication, and types of drug, might have potential impacts on the differences between un-medicated MDD patients and medicated MDD patients. Therefore, we will explore the potential impacts of medication status in our future work.

In summary, we propose a data-driven analytical approach allowing the investigation of dynamic alterations in whole-brain networks between patients with MDD and healthy controls across cohorts. Based on the HMM, we identified the brain microstates, each of which can be characterized by the patterns of mean activation and by the transitions probability between the active states. Our findings reveal that there are the reorganization of intrinsic brain states at time scales for MDD, the special module of transitions between large-scale brain networks for MDD, and multiple transitions pathways between MDD patients and healthy controls. In particular, the special community for MDD is characterized by decreased activation and connectivity in DMN, which contrasts significantly with increased activation in healthy controls. Our findings provide new insights into the large-scale dynamic circuit organization of the brain in MDD and suggest that brain dynamics should remain a prime target for further MDD research, especially regarding the intrinsic states underlying brain activity.

Funding Information This work was supported in part by the National Natural Science Foundation of China (Grant Number:61976209, 61906188 and 81701785), in part by the International Collaboration Key Project of Chinese Academy of Sciences (CAS) (Grant Number: 173211KYSB20190024), in part by the Fundamental Research Funds fotr the Central Universities (Grant Number: SWU118065), and in part by the Strategic Priority Research Program of CAS (Grant Number: XDB32040000).

Compliance with Ethical Standards

Competing Interests The authors declare that they have no competing interests.

Data and Code Availability The datasets generated and/or analyzed as well as code used during the current study are available upon reasonable request.

References

1. Kennedy SH (2008) Core symptoms of major depressive disorder: relevance to diagnosis and treatment. Dialogues Clin Neurosci 10: 271–277
2. Ng CWM, How CH, Ng YP (2016) Major depression in primary care: Making the diagnosis. Singap Med J 57:591–597
3. Ferrari AJ, Charlson FJ, Norman RE, Patten SB, Freedman G, Murray CJL, Vos T, Whiteford HA (2013) Burden of depressive disorders by country, sex, age, and year: findings from the global burden of disease study 2010. PLoS Med 10:e1001547
4. Yan C-G, Chen X, Li L, Castellanos FX, Bai TJ, Bo QJ, Cao J, Chen GM et al (2019) Reduced default mode network functional connectivity in patients with recurrent major depressive disorder. Proc Natl Acad Sci U S A 116:9078–9083
5. Bora E, Harrison BJ, Yücel M, Pantelis C (2013) Cognitive impairment in euthymic major depressive disorder: a meta-analysis. Psychol Med 43:2017–2026
6. McIntyre RS, Cha DS, Soczynska JK, Woldeyohannes HO, Gallaugher LA, Kudlow P, Alsuwaidan M, Baskaran A (2013) Cognitive deficits and functional outcomes in major depressive disorder: determinants, substrates, and treatment interventions. Depress Anxiety 30:515–527
7. Lam RW, Kennedy SH, Mclntyre RS, Khullar A (2014) Cognitive dysfunction in major depressive disorder: effects on psychosocial functioning and implications for treatment. Can J Psychiatr 59:649–654
8. Sheline YI, Price JL, Yan Z, Mintun MA (2010) Resting-state functional MRI in depression unmasks increased connectivity between networks via the dorsal nexus. Proc Natl Acad Sci U S A 107:11020–11025
9. Zeng L-L, Shen H, Liu L, Wang L, Li B, Fang P, Zhou Z, Li Y et al (2012) Identifying major depression using whole-brain functional connectivity: a multivariate pattern analysis. Brain 135:1498–1507
10. Helm K, Viol K, Weiger TM, Tass PA, Grefkes C, del Monte D, Schiepek G (2018) Neuronal connectivity in major depressive disorder: a systematic review. Neuropsychiatr Dis Treat 14:2715–2737
11. Hutchison RM, Womelsdorf T, Allen EA, Bandettini PA, Calhoun VD, Corbetta M, Della Penna S, Duyn JH et al (2013) Dynamic functional connectivity: promise, issues, and interpretations. Neuroimage 80:360–378
12. Liao X et al (2015) Spontaneous functional network dynamics and associated structural substrates in the human brain. Front Hum Neurosci 9:478
13. Fong AHC, Yoo K, Rosenberg MD, Zhang S, Li CSR, Scheinost D, Constable RT, Chun MM (2019) Dynamic functional connectivity during task performance and rest predicts individual differences in attention across studies. Neuroimage 188:14–25
14. Liao W, Chen H, Li J, Ji GJ, Wu GR, Long Z, Xu Q, Duan X et al (2019) Endless fluctuations: temporal dynamics of the amplitude of low frequency fluctuations: temporal dynamics of the amplitude of low frequency fluctuations. IEEE Trans Med Imaging 38:2523–2532
15. Deco G, Jirsa VK, McIntosh AR (2011) Emerging concepts for the dynamical organization of resting-state activity in the brain. Nat Rev Neurosci 12:43–56
16. Gu S, Betzel RF, Mattar MG, Cieslak M, Delio PR, Grafton ST, Pasqualetti F, Bassett DS (2017) Optimal trajectories of brain state transitions. Neuroimage 148:305–317
17. Lin P, Yang Y, Gao J, de Pisapia N, Ge S, Wang X, Zuo CS, Jonathan Levitt J et al (2017) Dynamic default mode network across different brain states. Sci Rep 7:46088
18. Damaraju E, Allen EA, Belger A, Ford JM, McEwen S, Mathalon DH, Mueller BA, Pearlson GD et al (2014) Dynamic functional connectivity analysis reveals transient states of dysconnectivity in schizophrenia. Neuroimage Clin 5:298–308
19. Du Y et al (2018) Dynamic functional connectivity impairments in early schizophrenia and clinical high-risk for psychosis. Neuroimage 180:632–645
20. Du Y et al (2016) Interaction among subsystems within default mode network diminished in schizophrenia patients: A dynamic connectivity approach. Schizophr Res 170:55–65
21. Yang S, Meng Y, Li J, Fan YS, du L, Chen H, Liao W (2019) Temporal dynamic changes of intrinsic brain activity in schizophrenia with cigarette smoking. Schizophr Res 210:66–72

22. Sheline YI, Raichle ME (2013) Resting state functional connectivity in preclinical Alzheimer's disease: a review. Biol Psychiatry 74: 340–347
23. de Haan W, van der Flier WM, Koene T, Smits LL, Scheltens P, Stam CJ (2012) Disrupted modular brain dynamics reflect cognitive dysfunction in Alzheimer's disease. Neuroimage 59:3085–3093
24. Li J, Duan X, Cui Q, Chen H, Liao W (2019) More than just statics: temporal dynamics of intrinsic brain activity predicts the suicidal ideation in depressed patients. Psychol Med 49:852–860
25. Nguyen TT, Kovacevic S, Dev SI, Lu K, Liu TT, Eyler LT (2017) Dynamic functional connectivity in bipolar disorder is associated with executive function and processing speed: a preliminary study. Neuropsychology 31:73–83
26. Preti MG, Bolton TA, van de Ville D (2017) The dynamic functional connectome: State-of-the-art and perspectives. Neuroimage 160:41–54
27. Wendling F, Ansari-Asl K, Bartolomei F, Senhadji L (2009) From EEG signals to brain connectivity: a model-based evaluation of interdependence measures. J Neurosci Methods 183:9–18
28. Allen EA, Damaraju E, Plis SM, Erhardt EB, Eichele T, Calhoun VD (2014) Tracking whole-brain connectivity dynamics in the resting state. Cereb Cortex 24:663–676
29. Vidaurre D, Abeysuriya R, Becker R, Quinn AJ, Alfaro-Almagro F, Smith SM, Woolrich MW (2018) Discovering dynamic brain networks from big data in rest and task. Neuroimage 180:646–656
30. Mokhtari F, Akhlaghi MI, Simpson SL, Wu G, Laurienti PJ (2019) Sliding window correlation analysis: Modulating window shape for dynamic brain connectivity in resting state. Neuroimage 189:655–666
31. Demirtaş M, Tornador C, Falcón C, López-Solà M, Hernández-Ribas R, Pujol J, Menchón JM, Ritter P et al (2016) Dynamic functional connectivity reveals altered variability in functional connectivity among patients with major depressive disorder. Hum Brain Mapp 37:2918–2930
32. Zhi D, Calhoun VD, Lv L, Ma X, Ke Q, Fu Z, du Y, Yang Y et al (2018) Aberrant dynamic functional network connectivity and graph properties in major depressive disorder. Front Psychiatry 9: 339
33. Kaiser RH, Whitfield-Gabrieli S, Dillon DG, Goer F, Beltzer M, Minkel J, Smoski M, Dichter G et al (2016) Dynamic resting-state functional connectivity in major depression. Neuropsychopharmacology 41:1822–1830
34. Hindriks R, Adhikari MH, Murayama Y, Ganzetti M, Mantini D, Logothetis NK, Deco G (2016) Can sliding-window correlations reveal dynamic functional connectivity in resting-state fMRI? Neuroimage 127:242–256
35. Leonardi N, van de Ville D (2015) On spurious and real fluctuations of dynamic functional connectivity during rest. Neuroimage 104: 430–436
36. Zalesky A, Breakspear M (2015) Towards a statistical test for functional connectivity dynamics. Neuroimage 114:466–470
37. Vidaurre D, Quinn AJ, Baker AP, Dupret D, Tejero-Cantero A, Woolrich MW (2016) Spectrally resolved fast transient brain states in electrophysiological data. Neuroimage 126:81–95
38. Vidaurre D, Smith SM, Woolrich MW (2017) Brain network dynamics are hierarchically organized in time. Proc Natl Acad Sci U S A 114:12827–12832
39. Stevner ABA, Vidaurre D, Cabral J, Rapuano K, Nielsen SFV, Tagliazucchi E, Laufs H, Vuust P et al (2019) Discovery of key whole-brain transitions and dynamics during human wakefulness and non-REM sleep. Nat Commun 10:1035
40. Quinn AJ, Vidaurre D, Abeysuriya R, Becker R, Nobre AC, Woolrich MW (2018) Task-evoked dynamic network analysis through hidden Markov modeling. Front Neurosci 12:603
41. Vidaurre D, Hunt LT, Quinn AJ, Hunt BAE, Brookes MJ, Nobre AC, Woolrich MW (2018) Spontaneous cortical activity transiently organises into frequency specific phase-coupling networks. Nat Commun 9:2987
42. Vidaurre D, Myers NE, Stokes M, Nobre AC, Woolrich MW (2019) Temporally unconstrained decoding reveals consistent but time-varying stages of stimulus processing. Cereb Cortex 29:863–874
43. Cheng W, Rolls ET, Qiu J, Yang D, Ruan H, Wei D, Zhao L, Meng J et al (2018) Functional connectivity of the precuneus in unmedicated patients with depression. Biol Psychiatry Cogn Neurosci Neuroimaging 3:1040–1049
44. Wei D et al (2020) The reductions in the subcallosal region cortical volume and surface area in major depressive disorder across the adult life span. Psychol Med 50(3):422–430
45. Tzourio-Mazoyer N, Landeau B, Papathanassiou D, Crivello F, Etard O, Delcroix N, Mazoyer B, Joliot M (2002) Automated anatomical labeling of activations in SPM using a macroscopic anatomical parcellation of the MNI MRI single-subject brain. Neuroimage 15:273–289
46. Newman MEJ (2006) Modularity and community structure in networks. Proc Natl Acad Sci U S A 103:8577–8582
47. Rubinov M, Sporns O (2010) Complex network measures of brain connectivity: uses and interpretations. Neuroimage 52:1059–1069
48. Liu CH, Li F, Li SF, Wang YJ, Tie CL, Wu HY, Zhou Z, Zhang D et al (2012) Abnormal baseline brain activity in bipolar depression: a resting state functional magnetic resonance imaging study. Psychiatry Res 203:175–179
49. Avery J, Drevets WC, Moseman S, Bodurka J, Barcalow J, Simmons WK (2013) Major depressive disorder is associated with abnormal interoceptive activity and functional connectivity in the insula. Biol Psychiatry 76:258–266
50. Wu X, He H, Shi L, Xia Y, Zuang K, Feng Q, Zhang Y, Ren Z et al (2019) Personality traits are related with dynamic functional connectivity in major depression disorder: A resting-state analysis. J Affect Disord 245:1032–1042
51. Supekar K, Cai W, Krishnadas R, Palaniyappan L, Menon V (2019) Dysregulated brain dynamics in a triple-network saliency model of schizophrenia and its relation to psychosis. Biol Psychiatry 85:60–69
52. Li C, Xia L, Ma J, Li S, Liang S, Ma X, Wang T, Li M et al (2019) Dynamic functional abnormalities in generalized anxiety disorders and their increased network segregation of a hyperarousal brain state modulated by insomnia. J Affect Disord 246:338–345
53. Schumacher J, Peraza LR, Firbank M, Thomas AJ, Kaiser M, Gallagher P, O'Brien JT, Blamire AM et al (2019) Dynamic functional connectivity changes in dementia with Lewy bodies and Alzheimer's disease. Neuroimage Clin 22:101812
54. Fu Z, Caprihan A, Chen J, du Y, Adair JC, Sui J, Rosenberg GA, Calhoun VD (2019) Altered static and dynamic functional network connectivity in Alzheimer's disease and subcortical ischemic vascular disease: shared and specific brain connectivity abnormalities. Hum Brain Mapp 40:3203–3221
55. Córdova-Palomera A, Kaufmann T, Persson K, Alnæs D, Doan NT, Moberget T, Lund MJ, Barca ML et al (2017) Disrupted global metastability and static and dynamic brain connectivity across individuals in the Alzheimer's disease continuum. Sci Rep 7:40268
56. Kaiser RH, Andrews-Hanna JR, Wager TD, Pizzagalli DA (2015) Large-scale network dysfunction in major depressive disorder: a meta-analysis of resting-state functional connectivity. JAMA Psychiatry 72:603–611
57. Hamilton JP, Farmer M, Fogelman P, Gotlib IH (2015) Depressive rumination, the default-mode network, and the dark matter of clinical neuroscience. Biol Psychiatry 78:224–230
58. Moreno-Ortega M, Prudic J, Rowny S, Patel GH, Kangarlu A, Lee S, Grinband J, Palomo T et al (2019) Resting state functional connectivity predictors of treatment response to electroconvulsive therapy in depression. Sci Rep 9:5071

59. Wang L et al (2019) Altered functional connectivity patterns of insular subregions in major depressive disorder after electroconvulsive therapy. Brain Imaging Behav. https://doi.org/10.1007/s11682-018-0013-z
60. Wei Q, Bai T, Chen Y, Ji G, Hu X, Xie W, Xiong Z, Zhu D et al (2018) The changes of functional connectivity strength in electroconvulsive therapy for depression: a longitudinal study. Front Neurosci 12:661
61. Bai T, Wei Q, Zu M, Xie W, Wang J, Gong-Jun J, Yu F, Tian Y et al (2019) Functional plasticity of the dorsomedial prefrontal cortex in depression reorganized by electroconvulsive therapy: Validation in two independent samples. Hum Brain Mapp 40: 465–473
62. Ji G-J, Liao W, Chen F-F, Zhang L, Wang K (2017) Low-frequency blood oxygen level-dependent fluctuations in the brain white matter: More than just noise: more than just noise. Sci Bull 62:656–657
63. Gawryluk JR, Mazerolle EL, D'Arcy RCN (2014) Does functional MRI detect activation in white matter? A review of emerging evidence, issues, and future directions: a review of emerging evidence, issues, and future directions. Front Neurosci 8:239
64. Li J, Biswal BB, Wang P, Duan X, Cui Q, Chen H, Liao W (2019) Exploring the functional connectome in white matter. Hum Brain Mapp 40:4331–4344
65. Ding Z, Huang Y, Bailey SK, Gao Y, Cutting LE, Rogers BP, Newton AT, Gore JC (2018) Detection of synchronous brain activity in white matter tracts at rest and under functional loading. Proc Natl Acad Sci U S A 115:595–600

Publisher's Note Springer Nature remains neutral with regard to jurisdictional claims in published maps and institutional affiliations.